The 9-Borataphenanthrene Anion

Tyler A. Bartholome,[a] Aishvaryadeep Kaur,[b] David J. D. Wilson,[b] Jason L. Dutton,[b] and Caleb D. Martin*,[a]

[a]Baylor University, Department of Chemistry and Biochemistry, One Bear Place #97348, Waco, TX 76798

[b]Department of Chemistry and Physics, La Trobe Institute for Molecular Science, La Trobe University, Melbourne, Victoria, Australia, 3086

KEYWORDS Boron heterocycles, boratabenzene, borataalkene, hydroboration

ABSTRACT: The 9-borataphenanthrene anion is easily accessed by deprotonation of a 9,10-dihydro-9-boraphenanthrene and its diverse reactivity is investigated. The carbon atom adjacent to boron is nucleophilic, and room temperature hydroboration occurs across the B=C bond. The π-manifold of the central BC_5 ring coordinates to chromium in an η^6 fashion while only the B=C bond binds η^2 to gold, indicating versatility of the 9-borataphenanthrene anion as a ligand. Supporting calculations rationalize the observed reactivity, and aromaticity is corroborated by nucleus-independent chemical shift (NICS) values.

INTRODUCTION

Alkenes and benzene rings are ubiquitous unsaturated hydrocarbyl functionalities. Isoelectronic and isosteric analogues of such species are of interest because the substitution of a C=C unit with a heteroatom-containing two π-electron unit results in the introduction of a dipole moment, which can be used to alter the physical and chemical properties of the molecule.[1-7] Boron-containing analogues of alkenes include aminoboranes and borataalkenes in which B-N and $[B{=}C]^-$ units serve as two π-electron systems (Figure 1).[1, 5, 8-9] The respective benzene analogues containing B-N or $[B{=}C]^-$ in place of two carbon atoms are 1,2-azaborines and boratabenzenes.[1-5, 10-14]

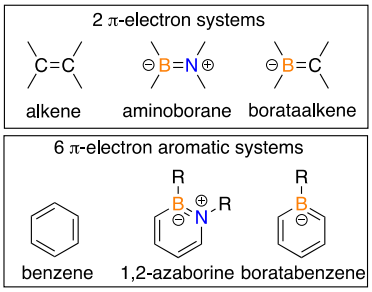

Figure 1. Isoelectronic relationship of an alkene and benzene to row two boron-containing species.

Boratabenzenes have been extensively studied as polyhaptic ligands for transition metals since their discovery in 1970 by Herberich and coworkers.[10-11, 13-53] The corresponding complexes and related compounds have been applied in fields that span olefin polymerization catalysis,[14, 30-32, 48, 54] asymmetric synthesis,[55-57] and single-ion magnets.[51] Research has primarily focused on monocyclic systems, with only three types of polycyclic boratabenzene-containing frameworks reported to date: 1-borataphthalenes,[58] 2-borataphthalenes,[29, 38, 59] and 9-borataanthracenes.[33, 60-62] (**A-C**, Figure 2). Analogues of phenanthrene with a boron atom at the 9-position are a particularly interesting target since they contain a distinct B=C moiety at the 9- and 10-positions that may be capable of acting as a borataalkene in contrast to the fused polycyclic boratabenzenes that are currently known. This expectation is founded on the known ability of phenanthrene to act as a biphenyl-substituted alkene, as evidenced by its alkene-like reactivity toward Br_2 via 9,10-dibromination,[63] ozonolysis at the 9- and 10-positions,[64-66] and diminished aromaticity in the central ring relative to the two peripheral rings.[67] Borataalkenes were first reported in 1972 by Rathke and Kow, who described them as boron-stabilized carbanions.[68] For nearly five decades, boratabenzene chemistry and borataalkene chemistry have remained separate fields. We herein report the first example of a 9-borataphenanthrene, a compound that features reactivity patterns of both boratabenzenes and borataalkenes.

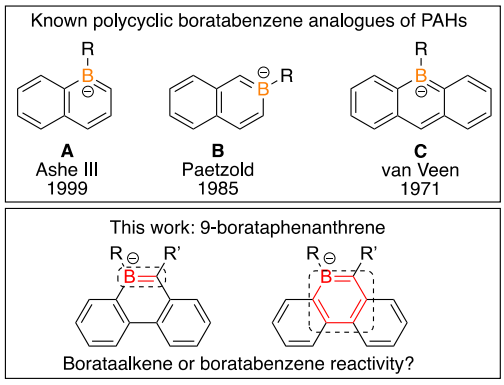

Figure 2. Known examples of boratabenzene analogues of polycyclic aromatic hydrocarbons and 9-borataphenanthrene disclosed in this work.

RESULTS AND DISCUSSION

Our group recently reported the synthesis of 9,10-dihydro-9-boraphenanthrene **D** via carbene insertion into the endocyclic B-C bond of 9-phenyl-9-borafluorene.[69] The compound bears a proton on an sp^3 carbon adjacent to a tricoordinate boron atom, making it a viable precursor to a boratabenzene-containing species by deprotonation. Potassium hexamethyldisilazide

(KHMDS) proved to be a suitable base to deprotonate **D** as confirmed by single crystal X-ray diffraction studies (Figure 3), and the resulting yellow borataphenanthrene **1** was isolated in high yield (86%, Scheme 1). The ^{1}H NMR spectrum of **1** lacks the aliphatic C-H proton at 3.88 ppm and features a diagnostic singlet at -0.01 ppm for the trimethylsilyl group, shifted downfield from -0.30 ppm for **D**. ^{11}B NMR spectroscopy revealed an upfield shift from 65.8 ppm for **D** to 40.4 ppm for **1**, consistent with boratabenzene and borataalkene species.[57-59, 70-76]

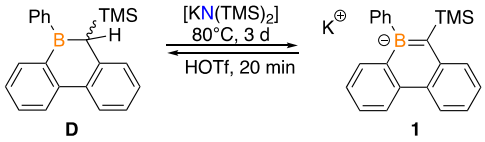

D **1**

Scheme 1. Interconversion of **D** with 9-borataphenanthrene **1**.

Theoretical calculations examining the electronic structure of **1** yield a geometry (as a free anion) in agreement with the X-ray diffraction structure (Table 1). The calculated HOMO is π-symmetric with the largest coefficients on the endocyclic B-C bond atoms, while the LUMO does not have any contribution at the boron atom (Figure 4). The Wiberg bond index (WBI) of the B-C bond in **1** is calculated to be 1.248, which indicates multiple B-C bond character in **1**. For comparison, the WBI is 0.929 for the analogous B-C single bond in precursor **D**. Nucleus independent chemical shift (NICS) scan calculations indicate that the boron-containing ring has significant aromatic character, with a NICS-scan minimum of -17 ppm at 1.3 Å above the plane of the ring. For comparison, the minima for benzene, the central ring of phenanthrene,[67] and 1-*H*-boratabenzene are -30 ppm, -21 ppm, and -26 ppm, respectively, all at 1.0 Å above the ring plane. These NICS-scan values indicate that incorporating boron into the ring, as well as fusing rings, reduces aromaticity. The NICS-scan calculations confirm aromatic character in the central ring, while the localization of the HOMO on the B=C functionality indicates that **1** can be described as either a dibenzo-fused boratabenzene or a biphenyl-substituted borataalkene. The borataalkene carbon atom has the largest partial negative NBO charge in **1** at -0.99, suggesting that this carbon has potential to act as a nucleophilic site.

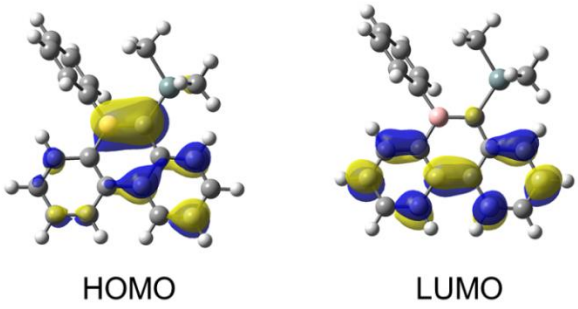

Figure 4. Frontier molecular orbitals of **1**.

To examine if 9-borataphenanthrene anion **1** acts as a nucleophile, in accordance with the calculated negative charge localized on the borataalkene carbon, protonation was attempted with triflic acid at room temperature. The reaction regenerated the protonated borataphenanthrene species **D** with potassium triflate as the byproduct (Scheme 1). C-alkylation was attempted by reaction with iodomethane[77-78] at room temperature (Scheme 2), resulting in a change in color from yellow to colorless. In situ ^{11}B NMR spectroscopy indicated a downfield shift in the boron resonance from 40.4 ppm to 67.2 ppm, indicative of the formation of a tricoordinate boron center, with conversion completed in 20 minutes. The isolated compound exhibits a diagnostic singlet at 1.86 ppm in its ^{1}H NMR spectrum that integrates in a 3:9 ratio with the trimethylsilyl singlet, confirming the addition of the methyl group to **1**. The structure of the compound was determined by X-ray crystallography to be the C-methylated derivative **2**, confirming carbon nucleophilicity (Figure 5).

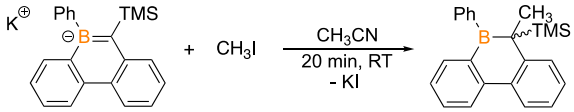

1 **2**

Scheme 2. Alkylation of **1** with iodomethane.

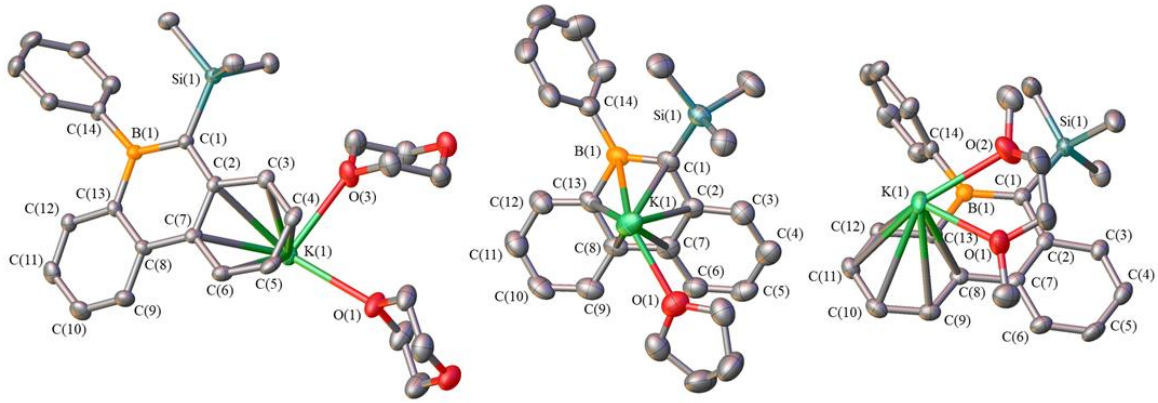

Figure 3. Solid-state structures of **1•dioxane**, **1•THF**, and **1•DME** (left to right). Hydrogen atoms are omitted for clarity, and thermal ellipsoids are drawn at the 50% probability level. The asymmetric units are displayed, and complete polymeric representations are shown in the SI (Figures S-60-62).

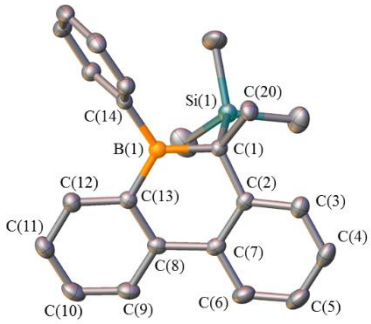

Figure 5. Solid-state structure of **2**. Hydrogen atoms are omitted for clarity, and thermal ellipsoids are drawn at the 50% probability level.

To determine if the borataalkene moiety of **1** can exhibit olefin-like behavior, hydroboration with pinacolborane (HBpin) was attempted at room temperature (Scheme 3). In situ ^{11}B NMR spectroscopy indicated the consumption of **1** and HBpin after 21 hours. The spectrum consisted of a broad singlet at 34.5 ppm and two distinct doublets; a major species at -11.1 ppm and minor species at -12.1, the latter consistent with hydride-substituted tetracoordinate boron centers. Both species were crystallized and identified as the *syn* (major) and *anti* (minor) isomers of the B=C hydroboration product (Figure 6). In their respective proton NMR spectra, broad quartets were observed at 2.62 and 2.69 ppm, with matching coupling constants to the doublets in the ^{11}B NMR spectrum (J = 90.0 Hz and 88.0 Hz) confirming the presence of a boron-bound hydride. This was further supported by an ^{1}H{^{11}B} experiment in which the quartets became singlets and a ^{11}B{^{1}H} experiment in which the doublets became singlets. This represents the first example of a B=C bond hydroboration in which the hydride is not bridged between the two boron centers and the first observation of an *anti* B=C bond hydroboration product.[74, 79-81] Allowing the reaction to proceed for longer periods of time showed a decrease in the intensity of the doublet at -11.1 ppm accompanied by an increase in the intensity of the doublet at -12.1 ppm in the in situ ^{11}B NMR spectra. Conducting variable-temperature ^{1}H NMR studies with a 1:1 mixture of ***syn*-3** and ***anti*-3** did not result in any interconversion of the two diastereomers; instead at 70 ºC, the intensity of the trimethylsilyl singlet for ***syn*-3** decreased with the emergence of a trimethylsilyl singlet at -0.01 ppm that corresponds to **1**. In addition, the Bpin methyl singlets for ***syn*-3** decreased in intensity and a singlet at 1.28 ppm corresponding to pinacolborane emerged. The methyl and trimethylsilyl singlets for ***anti*-3**, however, remained unchanged, thus confirming that the *syn* diastereomer, ***syn*-3**, is capable of thermal *syn* elimination of HBpin in a reverse hydroboration process while ***anti*-3** is not. Calculation of the reaction pathway shows that ***syn*-3** lies 11 kJ/mol below the starting materials, and isomerization to ***anti*-3** is a further 17 kJ/mol lower in energy. Modeling a simplified system bearing an -SiH_3 group on **1** showed that the transition state barrier for the conversion of **1** to ***syn*-3** is 84 kJ/mol (ΔG), and the reverse barrier is similar in magnitude for the model system at 85 kJ/mol. These data and the relatively flat ΔG of reaction at 11 kJ/mol are consistent with back-conversion of ***syn*-3** to **1** at elevated temperatures, driven by entropy. The ability of **1** to undergo hydroboration presents a potential new route to geminal bis(boron)-functionalized organic species.

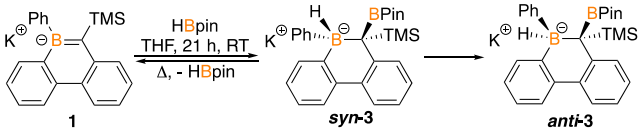

Scheme 3. Hydroboration of **1** with pinacolborane to produce diastereomers ***syn*-3** and ***anti*-3** (pin = pinacolate).

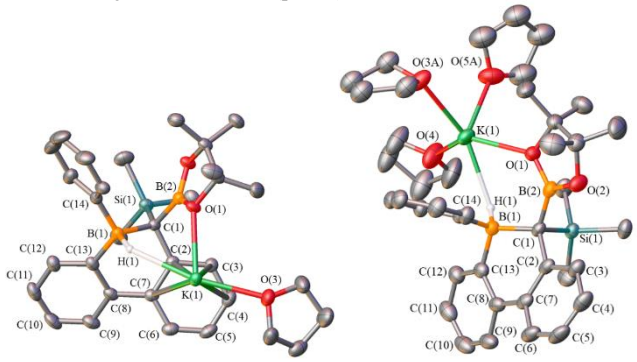

Figure 6. Solid-state structures of ***syn*-3** and ***anti*-3**. Hydrogen atoms (except for boron-bound hydrides) and non-coordinated solvates are omitted for clarity, and thermal ellipsoids are drawn at the 50% probability level. For disordered atoms, only the component with the highest occupancy is shown. The complete dimeric representation of ***syn*-3** is shown in the SI (Figure S-59).

The nucleophilicity at carbon and addition reactivity with HBpin provide evidence for a borataalkene description of **1**. Given the resemblance of the HOMO on the B=C bond to the HOMO of an olefin, we postulated that η^2 coordination with the π-bond could occur, reminiscent of an olefin.[82-84] Reaction of **1** with $(Ph_3P)AuCl$ at room temperature resulted in a color change from yellow to colorless (Scheme 4), and in situ ^{31}P{^{1}H} NMR spectroscopy showed the emergence of a singlet at 39.7 ppm along with the disappearance of the singlet at 33.2 ppm corresponding to $(Ph_3P)AuCl$ with the reaction complete in an hour. The in situ ^{11}B NMR spectrum showed a single broad peak at 42.4 ppm, slightly downfield from **1** (40.4 ppm). Single-crystal X-ray crystallography identified the product as the η^2-borataalkene complex **1•AuPPh$_3$** (Figure 7). The solid-state structure of **1•AuPPh$_3$** is disordered but clearly reveals that the gold center preferentially occupies a position closer to the borataalkene carbon rather than boron (88% site occupancy). The gold center is closer to the borataalkene carbon than to boron [Au-C = 2.188(7) Å] vs. Au-B = 2.427(8) Å], consistent with known examples of η^2-borataalkene complexes.[9, 85] Theoretical calculations reproduce this trend, with Au-C and Au-B bond distances of 2.227 and 2.491 Å, respectively. The geometry about the gold(I) center in **1•AuPPh$_3$** is approximately linear with respect to the borataalkene carbon as shown by its P-Au-C bond angle of 172.1(2)º. The ligand geometries about the borataalkene boron and carbon centers remain trigonal planar with angular sums of 359.6(9)º and 359.0(8)º. This is a unique borataalkene metal complex as it is the only example that originates from a free borataalkene. The only other species reported are of early transition metals and are prepared by modification of pre-existing ligands.[9, 85]

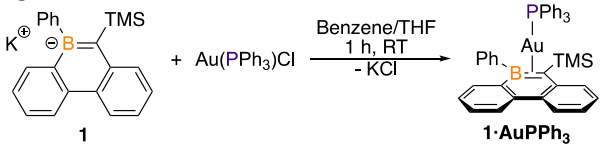

Scheme 4. Reaction of **1** with $(Ph_3P)AuCl$ to produce η^2-borataalkene complex **1•AuPPh$_3$**.

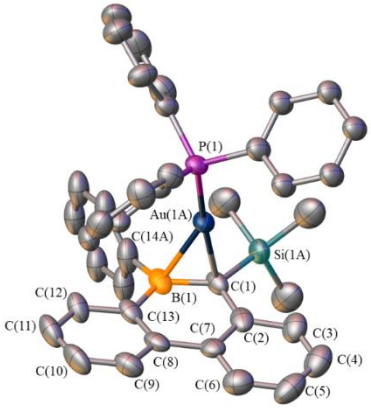

Figure 7. Solid-state structure of **1•AuPPh3**. Hydrogen atoms are omitted for clarity, and thermal ellipsoids are drawn at the 50% probability level. For disordered atoms, only the component with the highest occupancy is shown. Selected bond distances (Å) and angles (º): Au(1A)-B(1) 2.427(8), Au(1A)-C(1) 2.188(7), Au(1A)-P(1) 2.2618(18), B(1)-Au(1A)-P(1) 146.8(2), C(1)-Au(1A)-P(1) 172.1(2).

With the borataalkene reactivity of **1** established, the boratabenzene character was investigated next. To determine if the central BC_5 ring in 9-borataphenanthrene **1** exhibits boratabenzene reactivity, complexation with chromium was attempted by reacting **1** with tris(acetonitrile)tricarbonylchromium at room temperature in THF (Scheme 5). Upon mixing, the solution color immediately changed from yellow to red. In situ ^{11}B NMR spectroscopy revealed an upfield shift of the boron resonance from 40.4 ppm to 30.5 ppm, consistent with the formation of an η^6-boratabenzene complex[49-50, 52] with complete conversion of **1** in 75 minutes. Coordination of dibenzo-18-crown-6 to the potassium ion allowed for the isolation and crystallographic characterization of the piano-stool complex **1•Cr(CO)3** (Figure 8). The borataphenanthrene ligand coordinates to the chromium center through the central BC_5 ring. The FT-IR spectrum of the piano-stool complex **1•Cr(CO)3** exhibits carbonyl stretching bands at 1903, 1821, and 1769 cm^{-1}, which are similar to the chromium boratabenzene complex $Na[(MeBC_5H_5)Cr(CO)_3]$ (υ_{CO} = 1910, 1820, 1776 cm^{-1}).[26] The η^6 complexation of the central boratabenzene ring of **1** is consistent with the aromatic character determined in the NICS-scan calculations.

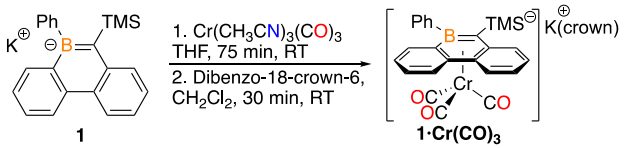

Scheme 5. Reaction of **1** with tris(acetonitrile)tricarbonylchromium to form η^6-boratabenzene complex **1•Cr(CO)3** (crown = dibenzo-18-crown-6).

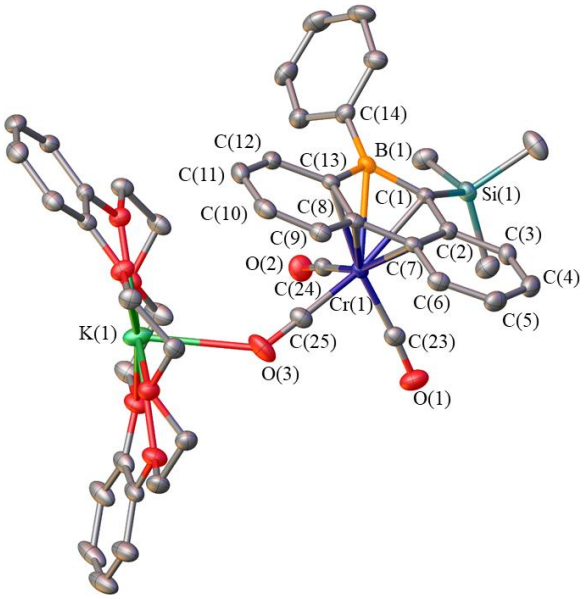

Figure 8. Solid-state structure of **1•Cr(CO)3**. Hydrogen atoms and dichloromethane solvate are omitted for clarity, and thermal ellipsoids are drawn at the 50% probability level. Selected bond distances (Å) and angles (º): B(1)-Cr(1) 2.410(4), C(1)-Cr(1) 2.294(3), C(2)-Cr(1) 2.306(4), C(7)-Cr(1) 2.294(3), C(8)-Cr(1) 2.329(3), C(13)-Cr(1) 2.349(3), Cr(1)-C(23) 1.821(4), C(23)-O(1) 1.171(5), Cr(1)-C(24) 1.813(4), C(24)-O(2) 1.163(5), Cr(1)-C(25) 1.809(4), C(25)-O(3) 1.174(5), O(3)-K(1) 2.849(4).

All compounds share the fused tricyclic framework, enabling a comparison of their common metrical parameters from X-ray diffraction data (Table 1). The structure of **1** was determined with three different solvates; THF, 1,4-dioxane, and dimethoxyethane (DME), with the closest contacts of the potassium cation with the borataphenanthrene anion differing in each. In the THF solvate, coordination of the potassium ion to the central boratabenzene ring occurs, while in the dioxane solvate, the potassium ion coordinates to the carbonaceous ring adjacent to the trimethylsilyl-substituted carbon, and in the DME solvate, the potassium ion coordinates to the carbonaceous ring adjacent to boron. The heteroatom bonds to the deprotonated carbon are notably shortened with the B-C bond of 1.541(3) Å of **D** contracting to 1.487(10)-1.495(2) Å in the structures of **1** and the C-Si bond contracting from 1.948(2) Å to 1.856(7)-1.8736(18) Å (Table 1). The boron-carbon and carbon-silicon bond distances of the methylated product are similar to **D** [**2**: B-C = 1.5481(18) Å and 1.9721(12) Å] while the metal complexes are similar to those of **1** [**1•AuPPh3**: B-C = 1.504(11) Å and C-Si = 1.891(12) Å, **1•Cr(CO)3**: B-C = 1.517(5) Å and C-Si = 1.888(4) Å] indicating that metal complexation has minimal effect on the bonding in the borataphenanthrene. The hydroboration products have significantly lengthened boron-carbon bonds [***syn*-3** = 1.702(3) Å, ***anti*-3** = 1.674(5) Å] that are consistent with quaternization of the boron center. In all the structures, there is minimal perturbation of the biphenyl framework.

CONCLUSION

The synthesis of the 9-borataphenanthrene anion enabled a reactivity study that revealed surprisingly diverse reaction modes. The feature compound readily undergoes protonation to

Table 1. Selected bond distances (Å) for **D**,[69] **1** (free anion, calculated), **1•dioxane**, **1•THF**, **1•DME**, **2**, ***syn*-3**, ***anti*-3**, **1•AuPPh$_3$**, and **1•Cr(CO)$_3$**.

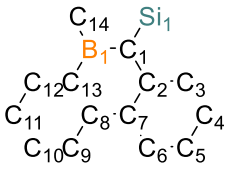

	D	1	1•dioxane	1•THF	1•DME	2	*syn*-3	*anti*-3	1•AuPPh$_3$	1•Cr(CO)$_3$
B(1)-C(1)	1.541(3)	1.497	1.495(2)	1.487(10)	1.489(3)	1.5481(18)	1.702(3)	1.674(5)	1.504(11)	1.517(5)
C(1)-Si(1)	1.948(2)	1.877	1.8736(18)	1.856(7)	1.8643(18)	1.9721(12)	1.9010(17)	1.906(3)	1.891(12)	1.888(4)
C(1)-C(2)	1.500(3)	1.453	1.450(2)	1.480(8)	1.456(2)	1.5129(16)	1.522(2)	1.525(4)	1.501(12)	1.441(5)
C(2)-C(3)	1.402(3)	1.432	1.434(2)	1.407(10)	1.429(2)	1.4052(18)	1.406(3)	1.412(5)	1.411(11)	1.444(5)
C(2)-C(7)	1.406(3)	1.448	1.444(2)	1.426(9)	1.440(3)	1.4182(18)	1.423(2)	1.415(5)	1.435(11)	1.449 (5)
C(3)-C(4)	1.372(3)	1.383	1.376(3)	1.382(10)	1.373(3)	1.382(2)	1.387(3)	1.385(5)	1.362(14)	1.357(5)
C(4)-C(5)	1.375(3)	1.407	1.397(3)	1.393(11)	1.392(3)	1.386(2)	1.388(3)	1.389(7)	1.376(15)	1.407(6)
C(5)-C(6)	1.370(3)	1.386	1.380(3)	1.367(10)	1.371(3)	1.381(2)	1.382(3)	1.372(6)	1.377(14)	1.364(5)
C(6)-C(7)	1.405(3)	1.417	1.415(2)	1.412(9)	1.416(3)	1.4087(18)	1.403(3)	1.412(5)	1.401(13)	1.436(5)
C(7)-C(8)	1.484(3)	1.466	1.471(2)	1.462(10)	1.463(2)	1.4839(18)	1.483(3)	1.491(5)	1.485(11)	1.468(5)
C(8)-C(9)	1.401(3)	1.421	1.418(2)	1.412(10)	1.419(3)	1.4095(18)	1.402(3)	1.406(5)	1.398(11)	1.431(5)
C(8)-C(13)	1.422(3)	1.430	1.419(2)	1.422(9)	1.421(2)	1.4170(17)	1.413(3)	1.409(5)	1.424(12)	1.429(5)
C(9)-C(10)	1.377(3)	1.387	1.370(3)	1.366(12)	1.380(3)	1.381(2)	1.389(3)	1.372(7)	1.377(13)	1.370(6)
C(10)-C(11)	1.379(3)	1.407	1.394(3)	1.382(10)	1.397(3)	1.388(2)	1.380(3)	1.386(7)	1.383(15)	1.411(6)
C(11)-C(12)	1.378(3)	1.387	1.375(3)	1.392(11)	1.376(3)	1.3846(19)	1.393(3)	1.389(5)	1.383(12)	1.353(6)
C(12)-C(13)	1.403(3)	1.419	1.420(2)	1.400(10)	1.419(2)	1.4108(18)	1.404(3)	1.398(5)	1.400(11)	1.441(5)
C(13)-B(1)	1.551(3)	1.560	1.553(3)	1.563(9)	1.562(3)	1.5496(18)	1.618(3)	1.605(5)	1.545(11)	1.546(5)
B(1)-C(14)	1.570(3)	1.594	1.603(3)	1.604(9)	1.601(3)	1.5782(17)	1.628(3)	1.636(4)	1.597(12)	1.586(6)

regenerate its charge-neutral precursor or methylation at carbon with iodomethane, consistent with the B=C bond polarization and borataalkene reactivity. Hydroboration of the B=C bond with pinacolborane demonstrated the potential of addition reactions in the system and provided a B=C hydroboration product that does not have a three-center two-electron bond with the hydride and boron atoms. Accordingly, this is also the first observation of an *anti* hydroboration product and provides a potential route to geminal bis(boron)-functionalized organic molecules. A unique η^2-borataalkene gold complex was synthesized and is the first example of a late metal borataalkene complex as well as the only example of an η^2-borataalkene complex prepared from the free anion. The 9-borataphenanthrene species coordinates to chromium in an η^6 fashion from the central BC_5 ring to underscore the diverse reactivity. Although several unusual transformations were disclosed in this manuscript, we are merely scratching the surface of the chemistry of the 9-borataphenanthrene anion. Overall the new class of compound demonstrates C-based nucleophilic, olefinic, and aromatic behavior and reactivity within a single heterocyclic ring system.

EXPERIMENTAL SECTION

General Considerations: All manipulations were performed under an inert atmosphere in a nitrogen-filled MBraun Unilab glove box or using standard Schlenk techniques. $CDCl_3$, C_6D_6, and CD_3CN for NMR spectroscopy were purchased from Cambridge Isotope Laboratories and dried by stirring for 3 days over CaH_2, distilling, and storing over molecular sieves. Dimethoxyethane was purchased from Acros Organics and dried by stirring for 3 days over CaH_2, distilling, and storing over molecular sieves. 1,4-Dioxane was purchased from Beantown Chemical and stored over molecular sieves. All other solvents were purchased from commercial sources as anhydrous grade, dried further using a JC Meyer Solvent System with dual columns packed with solvent-appropriate drying agents, and stored over molecular sieves. 9-Phenyl-9-borafluorene and (Ph_3P)AuCl were prepared by the literature procedures.[86-87] The following reagents were purchased from the listed sources and used as received: Trimethylsilyldiazomethane 2 M solution in hexanes (Acros Organics), pinacolborane (Acros Organics), triflic acid (Beantown Chemical), potassium bis(trimethylsilyl)amide (Aldrich) tris(acetonitrile)tricarbonylchromium (Aldrich), dibenzo-18-crown-6 (TCI). Iodomethane was purchased from Acros Organics and stored over molecular sieves. Multinuclear NMR spectra (^{1}H, ^{1}H{^{11}B}, ^{13}C{^{1}H}, ^{11}B, ^{11}B{^{1}H}, ^{31}P{^{1}H}) were recorded on a Bruker Ascend 400 MHz instrument. High resolution mass spectra (HRMS) were obtained at the Baylor University Mass Spectrometry Center on a Thermo Scientific LTQ Orbitrap Discovery spectrometer using ESI or at the University of Texas at Austin Mass Spectrometry Center on a Micromass Autospec Ultima spectrometer using CI. Melting points were measured with a Thomas Hoover Uni-melt capillary melting point apparatus and are uncorrected. FT-IR spectra were recorded on a Bruker Alpha ATR FT-IR spectrometer on solid samples. Single crystal X-ray diffraction data were collected on a Bruker Apex II-CCD detector using Mo-Kα radiation (λ = 0.71073 Å). Crystals were selected under paratone oil, mounted on MiTeGen micromounts, and immediately placed in a cold stream of N_2. Structures were solved and refined using SHELXTL and figures produced using OLEX2.[88-89]

Computational Methods: Unless noted, all calculations were performed with the Gaussian 16 program.[90] Geometry optimizations were carried out in a THF solvent forcefield using

B3LYP-D3(BJ)[91] with a def2-SVP basis set.[92] Frequency calculations were performed analytically at the same level of theory to characterize the stationary points as minima or transition states. NBO analysis was carried out with NBO 6.0.[93] Plots of molecular orbitals were obtained by performing MO analysis at B3LYP-D3(BJ)/def2-SVP in THF solvent. NICS scan calculations were carried out with the AROMA program[67, 94-96] coupled to Gaussian. NICS calculations were carried out with the B3LYP[97-98] method, def2-TZVP basis set,[92] and THF solvation.

Synthesis of **D**: **D** was prepared using a modified version of the literature procedure to accommodate a larger scale.[69] Trimethylsilyldiazomethane (2 M in hexanes, 2.67 mL, 5.34 mmol) was added dropwise to a solution of 9-phenyl-9-borafluorene (1.12 g, 4.65 mmol) in *n*-pentane (25 mL) while stirring at room temperature. The reaction mixture was then stirred for an additional hour, after which the volatile components were removed *in vacuo*. The resulting solid was then recrystallized from *n*-pentane at -35 ºC to yield **D** as a colorless solid. Yield: 1.15 g (75%). The characterization details match the literature data.[69]

Synthesis of **D** from **1**: A solution of triflic acid (25 µL, 0.28 mmol) in THF (2.5 mL) was added dropwise to a solution of **1** (102 mg, 0.281 mmol) in THF (2.5 mL) while stirring at room temperature. After 15 minutes of stirring, the volatile components were removed *in vacuo*, and the residue was extracted with benzene (3 mL). The supernatant was then filtered and lyophilized to yield **D** as a white powder. Yield: 72 mg (79%). The characterization details match the literature data.[69]

Synthesis of **1**: A solution of potassium bis(trimethylsilyl)amide (0.630 g, 3.16 mmol) in benzene (15 mL) was added dropwise to a solution of **D** (0.964 g, 2.95 mmol) in benzene (5 mL) while stirring at room temperature. The resulting yellow solution was then transferred to a pressure tube with a Teflon cap and heated at 80 ºC for 3 d, resulting in the formation of a yellow precipitate. The precipitate was collected by vacuum filtration, washed with additional benzene (40 mL), and dried *in vacuo* to yield **1** as a yellow powder. Yield: 0.922 g (86%). m.p. 99-102 ºC. Crystals for X-ray diffraction studies were grown by vapor diffusion of *n*-pentane into a 1,4-dioxane solution of **1** (**1•dioxane**), by vapor diffusion of *n*-pentane into a THF solution of **1** (**1•THF**), or by vapor diffusion of hexanes into a dimethoxyethane solution of **1** (**1•DME**). ^{1}H NMR (400 MHz, CD_3CN): δ 8.59 (d, *J* = 8.0 Hz, 1H), 8.55 (dd, *J* = 8.0, 2.5 Hz, 1H), 7.84 (dd, *J* = 8.5, 1.0 Hz, 1H), 7.64 (dd, *J* = 7.5, 1.5 Hz, 1H), 7.50-7.48 (m, 2H), 7.39-7.35 (m, 1H), 7.29-7.25 (m, 2H), 7.20-7.11 (m, 3H), 6.91-6.87 (m, 1H), -0.01 (s, 9H); ^{13}C{^{1}H} NMR (101 MHz, CD_3CN): δ 148.13, 138.50, 134.99, 134.45, 128.63, 127.82, 126.67, 125.04, 124.61, 124.46, 124.11, 122.53, 122.50, 115.49, 4.61; ^{11}B NMR (128 MHz, CD_3CN): δ 40.4; FT-IR (cm^{-1} (ranked intensity)): 1467 (9), 1417 (15), 1298 (6), 1256 (14), 1243 (8), 1229 (13), 930 (7), 863 (10), 828 (1), 761 (2), 748 (3), 727 (5), 710 (4), 676 (12), 622 (11); high-resolution mass spectrometry (HRMS) electrospray ionization (ESI): calcd for $C_{22}H_{22}BSi$ [M]$^-$, 325.1583; found, 325.1578.

Synthesis of **2**: Iodomethane (55 µL, 0.88 mmol) was added dropwise to a solution of **1** (107 mg, 0.293 mmol) in acetonitrile (3 mL) while stirring at room temperature. After 20 minutes, the reaction mixture was extracted with *n*-pentane (3 × 5 mL). The volatile components were then evaporated *in vacuo* from the *n*-pentane extract to afford **2** as a colorless oil, which was lyophilized from benzene to produce a white powder. This powder was then further purified by recrystallization from *n*-pentane at -35 ºC. Yield: 63 mg (63%). d.p. 82 ºC. Crystals for X-ray diffraction studies were grown by storing an *n*-pentane solution of **2** at -35 ºC. ^{1}H NMR (400 MHz, C_6D_6): δ 8.10 (t, *J* = 8.0 Hz, 2H), 7.84 (dd, *J* = 7.5, 1.0 Hz, 1H), 7.43-7.39 (m, 4H), 7.34-7.21 (m, 5H), 7.16-7.12 (m, 1H), 1.86 (s, 3H), -0.33 (s, 9H); ^{13}C{^{1}H} NMR (101 MHz, C_6D_6): δ 144.37, 143.82, 136.99, 134.28, 133.62, 132.21, 127.44, 127.41, 126.75, 126.60, 125.55, 124.56, 123.23, 17.91, -1.07; ^{11}B NMR (128 MHz, C_6D_6): δ 67.2; FT-IR (cm^{-1} (ranked intensity)): 1591 (15), 1437 (13), 1247 (4), 1226 (12), 950 (14), 835 (1), 766 (8), 752 (5), 744 (7), 732 (2), 707 (3), 690 (11), 671 (6), 663 (9), 636 (10); high-resolution mass spectrometry (HRMS) chemical ionization (CI): calcd for $C_{23}H_{25}BSi$ [M]$^+$, 340.1819; found, 340.1821.

Synthesis of ***syn*-3**: Pinacolborane (212 µL, 1.46 mmol) was added to a solution of **1** (354 mg, 0.972 mmol) in THF (5 mL) while stirring at room temperature. After 21 hours of stirring, the solution was concentrated to a volume of 2 mL, resulting in the formation of a cloudy yellow precipitate. The precipitate was isolated by decantation and dried *in vacuo* to yield ***syn*-3** as a pale-yellow powder. Yield: 308 mg (64%, minimum 7:1 diastereomer ratio). d.p. 167 ºC. Crystals for X-ray diffraction studies were grown by slow evaporation of a solution of ***syn*-3** in THF/benzene (5:1). ^{1}H NMR (400 MHz, CD_3CN): δ 7.57-7.55 (m, 1H), 7.43 (d, *J* = 7.5 Hz, 1H), 7.20-7.17 (m, 2H), 7.01-6.93 (m, 4H), 6.88 (td, *J* = 7.5, 1.5 Hz, 1H), 6.80 (td, *J* = 7.0, 1.5 Hz, 1H), 6.67-6.64 (m, 3H), 2.62 (q, *J* = 90.0 Hz, 1H), 0.87 (s, 6H), 0.69 (s, 6H), -0.08 (s, 9H); ^{1}H{^{11}B} NMR (400 MHz, CD_3CN): δ 7.57-7.55 (m, 1H), 7.43 (d, *J* = 7.5 Hz, 1H), 7.20-7.18 (m, 2H), 7.00-6.93 (m, 4H), 6.88 (td, *J* = 7.0, 1.5 Hz, 1H), 6.81-6.78 (m, 1H), 6.68-6.65 (m, 3H), 2.62 (s, 1H), 0.87 (s, 6H), 0.68 (s, 6H), -0.08 (s, 9H); ^{13}C{^{1}H} NMR (101 MHz, CD_3CN): δ 151.88, 142.70, 136.09, 134.35, 131.16, 126.13, 125.52, 125.45, 125.34, 124.02, 123.76, 122.95, 122.78, 81.31, 25.39, 24.50, 2.69; ^{11}B NMR (128 MHz, CD_3CN): δ 34.5 (s, br), -11.1 (d); ^{11}B{^{1}H} NMR (128 MHz, CD_3CN): δ 34.9 (s, br), -11.1 (s); FT-IR (cm^{-1} (ranked intensity)): 2974 (9), 1426 (10), 1297 (6), 1241 (4), 1140 (2), 973 (7), 891 (14), 828 (1), 762 (13), 737 (3), 716 (5), 674 (8), 620 (15), 600 (12), 510 (11); high-resolution mass spectrometry (HRMS) electrospray ionization (ESI): calcd for $C_{28}H_{35}B_2O_2Si$ [M]$^-$, 453.2592; found, 453.2614.

Synthesis of ***anti*-3**: Pinacolborane (52 µL, 0.36 mmol) was added to a solution of **1** (87 mg, 0.24 mmol) in THF (3 mL) while stirring at room temperature. After 17 days of stirring, the volatile components were removed *in vacuo* to produce a colorless oil. The oil was then redissolved in a mixture of THF (1 mL) and *n*-pentane (2 mL) and recrystallized at -35 ºC to yield colorless crystals of ***anti*-3**. Yield: 72 mg (61%). d.p. 151 ºC. Crystals for X-ray diffraction studies were grown by storing an *n*-pentane/THF (2:1) solution of ***anti*-3** at -35 ºC. ^{1}H NMR (400 MHz, CD_3CN): δ 7.66-7.64 (m, 1H), 7.56-7.53 (m, 1H), 7.44-7.40 (m, 1H), 7.26 (s, br, 1H), 7.13-7.12 (m, 2H), 7.00-6.92 (m, 2H), 6.85-6.81 (m, 2H), 6.70-6.66 (m, 2H), 6.64-6.59 (m, 1H), 2.69 (q, br, *J* = 88.0 Hz, 1H), 0.98 (s, 6H), 0.82 (s, 6H), -0.34 (s, 9H); ^{1}H{^{11}B} NMR (400 MHz, CD_3CN): δ 7.66-7.64 (m, 1H), 7.56-7.53 (m, 1H), 7.44-7.40 (m, 1H), 7.27-7.24 (m, 1H), 7.14-7.11 (m, 2H), 7.00-6.92 (m, 2H), 6.86-6.81 (m, 2H), 6.70-6.66 (m, 2H), 6.64-6.60 (m, 1H), 2.68 (s, 1H), 0.98 (s, 6H), 0.82 (s, 6H), -0.34 (s, 9H); ^{13}C{^{1}H} NMR (101 MHz, CD_3CN): δ 141.10, 135.44, 135.37, 126.13, 125.82, 125.34, 124.27, 123.80, 123.28, 122.72, 122.69, 81.39, 25.65, 25.52, 0.63; ^{11}B NMR (128 MHz, CD_3CN): δ 35.4 (s, br), -12.1 (d); ^{11}B{^{1}H} NMR (128 MHz, CD_3CN): δ 35.1 (s, br), -12.1 (s); FT-IR (cm^{-1} (ranked intensity)): 2975 (12), 1477 (9), 1425 (11), 1371 (15),

1303 (6), 1238 (4), 1143 (3), 1023 (14), 972 (8), 833 (1), 742 (2), 712 (7), 677 (5), 620 (10), 596 (13); high-resolution mass spectrometry (HRMS) electrospray ionization (ESI): calcd for $C_{28}H_{35}B_2O_2Si$ $[M]^-$, 453.2592; found, 453.2521.

Synthesis of **1•AuPPh$_3$**: A solution of $(Ph_3P)AuCl$ (52 mg, 0.11 mmol) in benzene (4 mL) was added to a solution of **1** (39 mg, 0.11 mmol) in THF (1 mL) while stirring at room temperature. After 60 minutes, the volatile components were evaporated *in vacuo* to produce a colorless oily residue, which was then extracted with benzene (10 mL). The benzene extract was then filtered and lyophilized to yield **1•AuPPh$_3$** as a white powder. Yield: 73 mg (88%). d.p. 57 ºC. Crystals for X-ray diffraction studies were grown by vapor diffusion of *n*-pentane into a toluene solution of **1•AuPPh$_3$.** ^{1}H NMR (400 MHz, $CDCl_3$): δ 8.53 (dd, *J* = 8.0, 1.0 Hz, 1H), 8.48 (d, *J* = 8.0 Hz, 1H), 8.06 (d, *J* = 8.0 Hz, 1H), 7.62-7.57 (m, 2H), 7.52-7.42 (m, 6H), 7.34-7.29 (m, 8H), 7.24-7.20 (m, 3H), 7.10-7.05 (m, 6H), 0.16 (s, 9H); $^{13}C\{^1H\}$ NMR (101 MHz, $CDCl_3$): δ 149.70, 143.20, 143.14, 141.33, 139.75, 134.70, 134.06 (d, *J* = 14.0 Hz), 132.77, 131.56, 131.53, 129.54, 129.17 (d, *J* = 11.0 Hz), 129.07, 129.01, 128.83, 126.46, 125.55, 125.27, 125.20, 124.73, 122.83, 122.12, 4.65; ^{11}B NMR (128 MHz, $CDCl_3$): δ 42.4; $^{31}P\{^1H\}$ NMR (162 MHz, $CDCl_3$): δ 39.7; FT-IR (cm^{-1} (ranked intensity)): 1476 (9), 1435 (5), 1243 (8), 1099 (7), 928 (10), 829 (3), 745 (6), 729 (12), 691 (1), 676 (14), 639 (13), 619 (11), 593 (15), 532 (2), 498 (4); high-resolution mass spectrometry (HRMS) electrospray ionization (ESI): calcd for $C_{40}H_{37}AuBKPSi$ $[M+K]^+$, 823.1798; found, 823.1802.

Synthesis of **1•Cr(CO)$_3$**: A solution of tris(acetonitrile)tricarbonylchromium (76 mg, 0.29 mmol) in THF (6 mL) was added dropwise to a solution of **1** (108 mg, 0.296 mmol) in THF (2 mL) while stirring at room temperature under low-light conditions. After 75 minutes, dibenzo-18-crown-6 (107 mg, 0.296 mmol) in dichloromethane (4 mL) was added to the reaction mixture. The reaction mixture was then stirred for an additional 30 minutes, after which the volatile components were evaporated *in vacuo*. The resulting solid was then washed with dichloromethane (1 mL) to yield **1•Cr(CO)$_3$** as a bright red powder. Yield: 189 mg (75%). d.p. 131 ºC. Crystals for X-ray diffraction studies were grown by vapor diffusion of a dichloromethane solution of **1•Cr(CO)$_3$** into toluene. ^{1}H NMR (400 MHz, CD_3CN): δ 8.75 (d, *J* = 8.5 Hz, 1H), 8.50 (d, *J* = 8.5 Hz, 1H), 8.37 (s, br, 1H), 7.83 (d, *J* = 8.5 Hz, 1H), 7.47-7.24 (m, 8H), 7.02 (t, *J* = 8 Hz, 1H), 6.95 (s, 8H), 4.14-4.12 (m, 8H), 3.92-3.90 (m, 8H), 0.13 (s, 9H); $^{13}C\{^1H\}$ NMR (101 MHz, CD_3CN): δ 147.83, 138.68, 135.75, 135.38, 133.81, 129.97, 129.29, 129.18, 127.34, 125.99, 124.47, 123.42, 122.33, 122.23, 122.10, 115.49, 112.29, 97.83, 70.01, 68.00, 4.53; ^{11}B NMR (128 MHz, CD_3CN): δ 30.5; FT-IR (cm^{-1} (ranked intensity)): 1903 (7), 1821 (13), 1769 (3), 1503 (5), 1453 (9), 1245 (2), 1211 (10), 1120 (4), 1061 (12), 942 (6), 830 (8), 743 (1), 702 (15), 683 (14), 634 (11); high-resolution mass spectrometry (HRMS) chemical ionization (CI): calcd for $C_{25}H_{23}BCrO_3Si$ $[M+H]^-$, 462.0915; found, 462.0912.

ASSOCIATED CONTENT

The following files are available free of charge.
Supporting information (PDF)
Crystal structure data (CIF)
Cartesian coordinates for calculated geometries (XYZ)

AUTHOR INFORMATION

Corresponding Author

Email: *caleb_d_martin@baylor.edu

Author Contributions

The manuscript was written through contributions of all authors. All authors have given approval to the final version of the manuscript.

ACKNOWLEDGMENT

We are grateful to the Welch Foundation (Grant No. AA-1846) and the National Science Foundation for a CAREER Award (Award No. 1753025) for their generous support of this work. We also thank the ARC (FT16010007, DP20010013) for funding. We thank Dr. Sam Yruegas and Dr. Kevin K. Klausmeyer for assistance with X-ray crystallography and Dr. Xianzhong Xu for assistance with $^1H\{^{11}B\}$ and $^{11}B\{^1H\}$ NMR spectroscopy. NCI, Intersect, and La Trobe University are acknowledged for generous allocations of computing time.

REFERENCES

1. Campbell, P. G.; Marwitz, A. J. V.; Liu, S.-Y., Recent Advances in Azaborine Chemistry. *Angew. Chem. Int. Ed.* **2012,** *51*, 6074-6092.
2. Bosdet, M. J. D.; Piers, W. E., B-N as a C-C substitute in aromatic systems. *Can. J. Chem.* **2009,** *87*, 8-29.
3. Giustra, Z. X.; Liu, S.-Y., The State of the Art in Azaborine Chemistry: New Synthetic Methods and Applications. *J. Am. Chem. Soc.* **2018,** *140* (4), 1184-1194.
4. Braunschweig, H.; Hörl, C.; Mailänder, L.; Radacki, K.; Wahler, J., Antiaromaticity to Aromaticity: From Boroles to 1,2-Azaborinines by Ring Expansion with Azides. *Chem. Eur. J.* **2014,** *20*, 9858-9861.
5. Bélanger-Chabot, G.; Braunschweig, H.; Roy, D. K., Recent Developments in Azaborinine Chemistry. *Eur. J. Inorg. Chem.* **2017**, 4353-4368.
6. Brown, P. A.; Martin, C. D.; Shuford, K. L., Aromaticity of unsaturated BEC_4 heterocycles (E = N, P, As, Sb, O, S, Se, Te). *Phys. Chem. Chem. Phys.* **2019,** *21*, 18458-18466.
7. Noguchi, M.; Suzuki, K.; Kobayashi, J.; Yurino, T.; Tsurugi, H.; Mashima, K.; Yamashita, M., Planar and Bent BN-Embedded p-Quinodimethanes Synthesized by Transmetalation of Bis(trimethylsilyl)-1,4-dihydropyrazines with Chloroborane. *Organometallics* **2018,** *37* (12), 1833-1836.
8. Pelter, A., Some chemistry of hindered organoboranes. *Pure Appl. Chem.* **1994,** *66* (2), 223-233.
9. Cook, K. S.; Piers, W. E.; Woo, T. K.; McDonald, R., Reactions of Bis(pentafluorophenyl)borane with $Cp_2Ta(=CH_2)CH_3$: Generation and Trapping of Tantalocene Borataalkene Complexes. *Organometallics* **2001,** *20*, 3927-3937.
10. Herberich, G. E.; Ohst, H., Borabenzene Metal Complexes. *Adv. Organomet. Chem.* **1986,** *25*, 199-236.
11. Fu, G. C., The Chemistry of Borabenzenes (1986-2000). *Adv. Organomet. Chem.* **2001,** *47*, 101-119.
12. Marwitz, A. J. V.; Matus, M. H.; Zakharov, L. N.; Dixon, D. A.; Liu, S.-Y., A Hybrid Organic/Inorganic Benzene. *Angew. Chem. Int. Ed.* **2009,** *48*, 972-977.
13. Cui, P.; Chen, Y., Boratabenzene rare-earth metal complexes. *Coord. Chem. Rev.* **2016,** *314*, 2-13.
14. Ashe, A. J., III; Al-Ahmad, S.; Fang, X., Boratabenzenes: from chemical curiosities to promising catalysts. *J. Organomet. Chem.* **1999,** *581*, 92-97.
15. Ashe, A. J., III; Shu, P., The 1-Phenylborabenzene Anion. *J. Am. Chem. Soc.* **1971,** *93* (7), 1804-1805.

16. Herberich, G. E.; Greiss, G.; Heil, H. F., A Novel Aromatic Boron Heterocycle as Ligand in a Transition Metal π-Complex. *Angew. Chem. Int. Ed.* **1970,** *9* (10), 805-806.
17. Herberich, G. E.; Greiss, G.; Heil, H. F.; Müller, J., Paramagnetic Borabenzene Cobalt Complexes. *Chem. Commun.* **1971**, 1328-1329.
18. Huttner, G.; Krieg, B., Structure of $(CH_3OBC_5H_5)_2Co$, a Derivative of the Aromatic Hydridoborinate Anion. *Angew. Chem. Int. Ed.* **1972,** *11* (1), 42-43.
19. Huttner, G.; Krieg, B.; Gartzke, W., Kristall- und Molekülstrukturen von zwei "Borabenzol"-Derivaten: Bis(1-methoxyborinato)kobalt und Bis(1-methylborinato)kobalt. *Chem. Ber.* **1972,** *105*, 3424-3436.
20. Herberich, G. E.; Becker, H. J., Tricarbonyl-(1-phenylborinato)manganese. *Angew. Chem. Int. Ed.* **1973,** *12* (9), 764-765.
21. Ashe, A. J., III; Meyers, E.; Shu, P.; Lehmann, T. V.; Bastide, J., Bis(1-substituted-borabenzene)iron Complexes. *J. Am. Chem. Soc.* **1975,** *97* (23), 6865-6866.
22. Herberich, G. E.; Becker, H. J.; Carsten, K.; Engelke, C.; Koch, W., Ein neuer Weg zu Alkalimetallborinaten. Synthesen von Ruthenium-, Osmium-, Rhodium- und Platin-Verbindungen mit Borinat-Liganden. *Chem. Ber.* **1976,** *109*, 2382-2388.
23. Herberich, G. E.; Koch, W., Paramagnetische Chrom-Komplexe des 1-Methyl- und 1-Phenylborinat-Ions. *Chem. Ber.* **1977,** *110*, 816-819.
24. Herberich, G. E.; Carsten, K., Derivate des Borabenzols XI. Neuartige Ringumwandlungen von Borinatoeisen-Komplexen. *J. Organomet. Chem.* **1978,** *144*, C1-C5.
25. Herberich, G. E.; Hessner, B.; Kho, T. T., Derivate des Borabenzols XV. Friedel-Crafts-Acetylierung Versus Ringgliedsubstitution an Tricarbonyl(1-methylborinato)mangan. *J. Organomet. Chem.* **1980,** *197*, 1-5.
26. Herberich, G. E.; Söhnen, D., Derivate des Borabenzols XVII. Tricarbonyl(1-methylborinato)chrom-Derivate. *J. Organomet. Chem.* **1983,** *254*, 143-147.
27. Herberich, G. E.; Boveleth, W.; Hessner, B.; Koch, W.; Raabe, E.; Schmitz, D., Derivate des Borabenzols XVIII. Vanadium-Komplexe des 1-Methyl- und 1-Phenylborinat-Ions. *J. Organomet. Chem.* **1984,** *265*, 225-235.
28. Herberich, G. E.; Becker, H. J.; Hessner, B.; Zelenka, L., Derivate des Borabenzols XIX. Die Darstellung von Dicarbonyl(1-methylborinato)cobalt, von Zwei (Borinato)(cyclobutadien)cobalt-Komplexen mit Unsubstituiertem Cyclobutadien-Liganden und von Di-μ-carbonyl-bis[(1-methylborinato)nickel]. *J. Organomet. Chem.* **1985,** *280*, 147-151.
29. Paetzold, P.; Finke, N.; Wennek, P.; Schmid, G.; Boese, R., 2-Boratanaphthalin-Anion als hexahapto-gebundener Ligand. *Z. Naturforsch.* **1986,** *41b*, 167-174.
30. Bazan, G. C.; Rodriguez, G.; Ashe, A. J., III; Al-Ahmad, S.; Müller, C., Aminoboratabenzene Derivatives of Zirconium: A New Class of Olefin Polymerization Catalysts. *J. Am. Chem. Soc.* **1996,** *118*, 2291-2292.
31. Bazan, G. C.; Rodriguez, G.; Ashe, A. J., III; Al-Ahmad, S.; Kampf, J. W., (Phenylboratabenzene)zirconium Complexes: Tuning the Reactivity of an Olefin Polymerization Catalyst. *Organometallics* **1997,** *16*, 2492-2494.
32. Barnhart, R. W.; Bazan, G. C.; Mourey, T., Synthesis of Branched Polyolefins Using a Combination of Homogeneous Metallocene Mimics. *J. Am. Chem. Soc.* **1998,** *120*, 1082-1083.
33. Lee, R. A.; Lachicotte, R. J.; Bazan, G. C., Zirconium Complexes of 9-Phenyl-9-borataanthracene. Synthesis, Structural Characterization, and Reactivity. *J. Am. Chem. Soc.* **1998,** *120*, 6037-6046.
34. Herberich, G. E.; Englert, U.; Fischer, A.; Ni, J.; Schmitz, A., Borabenzene Derivatives. 29. Synthesis and Structural Diversity of Bis(boratabenzene)scandium Complexes. Structures of $[ScCl(C_5H_5BMe)_2]_2$, $[ScCl(3,5\text{-}Me_2C_5H_3BNMe_2)_2]_2$, and $ScCl[3,5\text{-}Me_2C_5H_3BN(SiMe_3)_2]_2$. *Organometallics* **1999,** *18*, 5496-5501.
35. Herberich, G. E.; Zheng, X.; Rosenplänter, J.; Englert, U., Borabenzene Derivatives. 30. Bis(1-methylboratabenzene) Compounds of Germanium, Tin, and Lead. First Structural Characterization of Facial Bonding of a Boratabenzene to a p-Element and the Structures of $Pb(C_5H_5BMe)_2$ and Its 2,2'-Bipyridine Adduct. *Organometallics* **1999,** *18*, 4747-4752.
36. Rogers, J. S.; Bu, X.; Bazan, G. C., Boratabenzene Complexes of Cr(III). *J. Am. Chem. Soc.* **2000,** *122*, 730-731.
37. Rogers, J. S.; Bu, X.; Bazan, G. C., Synthesis, Characterization, and Reactivity of Chromium Boratabenzene Complexes. *Organometallics* **2000,** *19*, 3948-3956.
38. Braunstein, P.; Cura, E.; Herberich, G. E., Heterometallic complexes and clusters with 2-boratanaphthalene ligands. *J. Chem. Soc., Dalton Trans.* **2001**, 1754-1760.
39. Zheng, X.; Wang, B.; Englert, U.; Herberich, G. E., Three Conformational Polymorphs of Di-μ-chlorotetrakis(1-methylboratabenzene)diyttrium: Synthesis, X-ray Structures, Quantum Chemical Calculations, and Lattice Energy Minimizations. *Inorg. Chem.* **2001,** *40*, 3117-3123.
40. Cui, P.; Chen, Y.; Zeng, X.; Sun, J.; Li, G.; Xia, W., Boratabenzene Derivatives of Divalent Samarium: Synthesis, Structures and Catalytic Reactivities of $(C_5H_5BXPh_2)_2Sm(THF)_2$ (X = N, P). *Organometallics* **2007,** *26*, 6519-6521.
41. Cui, P.; Chen, Y.; Li, G.; Xia, W., An ansa-Heteroborabenzene Divalent Lanthanide Amide through C-H Bond Cleavage. *Angew. Chem. Int. Ed.* **2008,** *47*, 9944-9947.
42. Yuan, Y.; Chen, Y.; Li, G.; Xia, W., Reactions of Boratabenzene Yttrium Complexes with $KN(SiMe_3)_2$: Salt Elimination and *π*-Ligand Displacement. *Organometallics* **2008,** *27*, 6307-6312.
43. Languérand, A.; Barnes, S. S.; Bélanger-Chabot, G.; Maron, L.; Berrouard, P.; Audet, P.; Fontaine, F. G., [(IMes)2Pt(H)(ClBC5H4SiMe3)]: a Borabenzene–Platinum Adduct with an Unusual Pt-Cl-B Interaction. *Angew. Chem. Int. Ed.* **2009,** *48*, 6695-6698.
44. Cui, P.; Chen, Y.; Zhang, Q.; Li, G.; Xia, W., Synthesis, and structural characterization of solvent-free divalent ytterbium bis(boratabenzene) and (cyclopentadienyl)(boratabenzene) complexes. *J. Organomet. Chem.* **2010,** *695*, 2713-2719.
45. Cui, P.; Chen, Y.; Li, G.; Xia, W., Versatile Reactivities of *ansa*-Heteroborabenzene Divalent Ytterbium Amide toward Alkali-Metal Salts and the Generation of Heterometallic Ytterbium--Alkali-Metal Boratabenzene Complexes. *Organometallics* **2011,** *30*, 2012-2017.
46. Pammer, F.; Lalancette, R. A.; Jäkle, F., Metallopolymers Featuring Boratabenzene Iron Complexes. *Chem. Eur. J.* **2011,** *17*, 11280-11289.
47. Yuan, Y.; Wang, X.; Li, Y.; Fan, L.; Xu, X.; Chen, Y.; Li, G.; Xia, W., Rapid Entry to Functionalized Boratabenzene Complexes through Metal-Induced Hydroboration at the Anionic 1-H-Boratabenzene Ligand. *Organometallics* **2011,** *30*, 4330-4341.
48. Wang, X.; Peng, W.; Cui, P.; Leng, X.; Xia, W.; Chen, Y., Synthesis and Catalytic Activity of Amido-Boratabenzene Complexes of Rare-Earth Metals and Zirconium and Chromium. *Organometallics* **2013,** *32*, 6166-6169.
49. Mushtaq, A.; Bi, W.; Légaré, M.-A.; Fontaine, F.-G., Synthesis and Reactivity of Novel Mesityl Boratabenzene Ligands and Their Coordination to Transition Metals. *Organometallics* **2014,** *33*, 3173-3181.
50. Pérez, V.; Barnes, S. S.; Fontaine, F.-G., Generation of Group VI Piano-Stool and Triple-Decker Complexes from $[(IMes)_2PtH(Cl\text{-}boratabenzene)]$ Species. *Eur. J. Inorg. Chem.* **2014**, 5698-5702.

51. Meng, Y.-S.; Wang, C.-H.; Zhang, Y.-Q.; Leng, X.-B.; Wang, B.-W.; Chen, Y.-F.; Gao, S., (Boratabenzene)(cyclooctatetraenyl) lanthanide complexes: a new type of organometallic single-ion magnet. *Inorg. Chem. Front.* **2016,** *3*, 828-835.
52. Perez, V.; Audet, P.; Bi, W.; Fontaine, F.-G., Phosphidoboratabenzene-rhodium(I) complexes as precatalysts for the hydrogenation of alkenes at room temperature and atmospheric pressure. *Dalton Trans.* **2016,** *45*, 2130-2137.
53. Krummenacher, I.; Schuster, J. K.; Braunschweig, H., Synthesis and Reactivity of Bora- and Borata-Benzenes. In *Patai's Chemistry of Functional Groups*, Marek, I.; Gandelman, M., Eds. 2019.
54. Janiak, C., Metallocene and related catalysts for olefin, alkyne and silane dimerization and oligomerization. *Coord. Chem. Rev.* **2006,** *250*, 66-94.
55. Tweddell, J.; Hoic, D. A.; Fu, G. C., First Synthesis and Structural Characterization of an Enantiomerically Pure Planar-Chiral Lewis Acid Complex. *J. Org. Chem.* **1997,** *62*, 8286-8287.
56. Herberich, G. E.; Ganter, B.; Pons, M., Borabenzene Derivatives. 27. From (-)-α-Pinene to the First Chiral Boratabenzene Salt. *Organometallics* **1998,** *17*, 1254-1256.
57. Herberich, G. E.; Englert, U.; Ganter, B.; Pons, M.; Wang, R., Borabenzene Derivatives. 28. Pinene-Fused Dihydroborinines, Boratabenzenes, and a Borabenzene-Pyridine Adduct. *Organometallics* **1999,** *18*, 3406-3413.
58. Ashe, A. J., III; Fang, X.; Kampf, J. W., Synthesis and Properties of 1-Substituted 1-Boratanaphthalenes. *Organometallics* **1999,** *18*, 466-473.
59. Herberich, G. E.; Cura, E.; Ni, J., A new synthetic route to 2-boratanaphthalenes. *Inorg. Chem. Commun.* **1999,** *2*, 503-506.
60. van Veen, R.; Bickelhaupt, F., The 9-mesityl-9-boraanthracene anion. *J. Organomet. Chem.* **1971,** *30*, C51-C53.
61. van Veen, R.; Bickelhaupt, F., Reactions of the 9-Mesityl-9-boraanthracene Anion. *J. Organomet. Chem.* **1974,** *77*, 153-165.
62. van Veen, R.; Bickelhaupt, F., Equilibrium CH-Acidity in Cyclohexylamine: The Aromatic 9-Mesityl-9-boraanthracene Anion. *J. Organomet. Chem.* **1974,** *74*, 393-403.
63. Mason, S. F., Reactivities of Aromatic Hydrocarbons. Part I. Bromination. *J. Chem. Soc.* **1958**, 4329-4333.
64. Bailey, P. S., The Ozonolysis of Phenanthrene in Methanol. *J. Am. Chem. Soc.* **1956,** *78* (15), 3811-3816.
65. Bailey, P. S.; Erickson, R. E., Diphenaldehyde. *Org. Synth.* **1961,** *41*, 41.
66. Copeland, P. G.; Dean, R. E.; McNeil, D., The Ozonolysis of Polycyclic Hydrocarbons. Part II. *J. Chem. Soc.* **1961**, 1232-1238.
67. Stanger, A., Nucleus-Independent Chemical Shifts (NICS): Distance Dependence and Revised Criteria for Aromaticity and Antiaromaticity. *J. Org. Chem.* **2006,** *71* (3), 883-893.
68. Rathke, M. W.; Kow, R., Generation of Boron-Stabilized Carbanions. *J. Am. Chem. Soc.* **1972,** *94* (19), 6854-6856.
69. Bartholome, T. A.; Bluer, K. R.; Martin, C. D., Successive Carbene Insertion into 9-Phenyl-9-Borafluorene. *Dalton Trans.* **2019,** *48*, 6319-6322.
70. Olmstead, M. M.; Power, P. P.; Weese, K. J.; Doedens, R. J., Isolation and X-ray Crystal Structure of the Boron Methylidenide Ion $[Mes_2BCH_2]^-$ (Mes = 2,4,6-$Me_3C_6H_2$): A Boron-Carbon Double Bonded Alkene Analogue. *J. Am. Chem. Soc.* **1987,** *109*, 2541-2542.
71. Herberich, G. E.; Schmidt, B.; Englert, U., Borabenzene Derivatives. 22. Synthesis of Boratabenzene Salts from 2,4-Pentadienylboranes. Structure of $[NMe_3Ph][C_5H_5BMe]$. *Organometallics* **1995,** *14*, 471-480.
72. Yu, J.; Kehr, G.; Daniliuc, C. G.; Erker, G., A Unique Frustrated Lewis Pair Pathway to Remarkably Stable Borata-Alkene Systems. *Eur. J. Inorg. Chem.* **2013**, 3312-3315.
73. Möbus, J.; Kehr, G.; Daniliuc, C. G.; Fröhlich, R.; Erker, G., Borata-alkene derivatives conveniently made by frustrated Lewis pair chemistry. *Dalton Trans.* **2014,** *43*, 632-638.
74. Kohrt, S.; Dachwitz, S.; Daniliuc, C. G.; Kehr, G.; Erker, G., Stabilized borata-alkene formation: structural features, reactions and the role of the counter cation. *Dalton Trans.* **2015,** *44*, 21032-21040.
75. Hoic, D. A.; Davis, W. M.; Fu, G. C., A Boron Analogue of Benzene: Synthesis, Structure, and Reactivity of 1-*H*-Boratabenzene. *J. Am. Chem. Soc.* **1995,** *117*, 8480-8481.
76. Bauer, J.; Braunschweig, H.; Hörl, C.; Radacki, K.; Wahler, J., Synthesis of Zwitterionic Cobaltocenium Borate and Borata-alkene Derivatives from a Borole-Radical Anion. *Chem. Eur. J.* **2013,** *19*, 13396-13401.
77. Pelter, A.; Williams, L.; Wilson, J. W., The Dimesitylboron Group in Organic Synthesis 2. The C-Alkylation of Alkyldimesitylboranes. *Tetrahedron Lett.* **1983,** *24* (6), 627-630.
78. Pelter, A.; Warren, L.; Wilson, J. W., Hindered Organoboron Groups in Organic Chemistry. 20. Alkylations and Acylations of Dimesitylboron Stabilised Carbanions. *Tetrahedron* **1993,** *49* (14), 2988-3006.
79. Kobayashi, A.; Suzuki, K.; Kitamura, R.; Yamashita, M., Formation of BCBH/BCBCl Four-Membered Rings by Complexation of Boron- and Nitrogen-Substituted Acetylene with Hydro-/Chloroboranes. *Organometallics* **2020,** *Accepted*.
80. Moquist, P.; Chen, G.-Q.; Mück-Lichtenfeld, C.; Bussmann, K.; Daniliuc, C. G.; Kehr, G.; Erker, G., α-CH acidity of alkyl-$B(C_6F_5)_2$ compounds - the role of stabilized borata-alkene formation in frustrated Lewis pair chemistry. *Chem. Sci.* **2015,** *6*, 816-825.
81. Wang, T.; Kehr, G.; Liu, L.; Grimme, S.; Daniliuc, C. G.; Erker, G., Selective Oxidation of an Active Intramolecular Amine/Borane Frustrated Lewis Pair with Dioxygen. *J. Am. Chem. Soc.* **2016,** *138*, 4302-4305.
82. Dávila, R. M.; Staples, R. J.; Fackler, Jr. J. P., Synthesis and Structural Characterization of $Au_4(MNT)(dppee)_2Cl_2 \bullet 1/4\ CH_2Cl_2$ (MNT = 1,2-Dicyanoethene-1,2-dithiolate-*S,S'*; dppee = *cis*-Bis(diphenylphosphino)ethylene): A Gold(I) Metal-Olefin Complex in Which the Olefin Orientation Relative to the Coordination Plane Involving the Metal Is Defined. *Organometallics* **1994,** *13*, 418-420.
83. Chambrier, I.; Rocchigiani, L.; Hughes, D. L.; Budzelaar, P. M. H.; Bochmann, M., Thermally Stable Gold(III) Alkene and Alkyne Complexes: Synthesis, Structures, and Assessment of the *trans*-Influence on Gold-Ligand Bond Enthalpies. *Chem. Eur. J.* **2018,** *24*, 11467-11474.
84. Cinellu, M. A.; Arca, M.; Ortu, F.; Stoccoro, S.; Zucca, A.; Pintus, A.; Maiore, L., Structural, Theoretical and Spectroscopic Characterisation of a Series of Novel Gold(I)-Norbornene Complexes Supported by Phenanthrolines: Effects of the Supporting Ligand. *Eur. J. Inorg. Chem.* **2019**, 4784-4795.
85. Cook, K. S.; Piers, W. E.; Rettig, S. J., Reactions of Bis(pentafluorophenyl)borane with $Cp_2Ta(=CH_2)CH_3$. *Organometallics* **1999,** *18*, 1575-1577.
86. Romero, P. E.; Piers, W. E.; Decker, S. A.; Chau, D.; Woo, T. K.; Parvez, M., η^1 versus η^5 Bonding Modes in Cp*Al(I) Adducts of 9-Borafluorenes. *Organometallics* **2003,** *22* (6), 1266-1274.
87. Bruce, M. I.; Nicholson, B. K.; Bin Shawkataly, O., Synthesis of Gold-Containing Mixed-Metal Cluster Complexes. *Inorg. Synth.* **1989,** *26*, 324-328.
88. Sheldrick, G. M., A short history of SHELX. *Acta Cryst.* **2008,** *A64* (Pt 1), 112-122.
89. Dolomanov, O. V.; Bourhis, L. J.; Gildea, R. J.; Howard, J. A. K.; Puschmann, H., OLEX2: a complete structure solution, refinement and analysis program. *J. Appl. Crystallogr.* **2009,** *42*, 339-341.

90. Frisch, M. J.; Trucks, G. W.; Schlegel, H. B.; Scuseria, G. E.; Robb, M. A.; Cheeseman, J. R.; Scalmani, G.; Barone, V.; Petersson, G. A.; Nakatsuji, H.; Li, X.; Caricato, M.; Marenich, A. V.; Bloino, J.; Janesko, B. G.; Gomperts, R.; Mennucci, B.; Hratchian, H. P.; Ortiz, J. V.; Izmaylov, A. F.; Sonnenberg, J. L.; Williams-Young, D.; Ding, F.; Lipparini, F.; Egidi, F.; Goings, J.; Peng, B.; Petrone, A.; Henderson, T.; Ranasinghe, D.; Zakrzewski, V. G.; Gao, J.; Rega, N.; Zheng, G.; Liang, W.; Hada, M.; Ehara, M.; Toyota, K.; Fukuda, R.; Hasegawa, J.; Ishida, M.; Nakajima, T.; Honda, Y.; Kitao, O.; Nakai, H.; Vreven, T.; Throssell, K.; Montgomery Jr., J. A.; Peralta, J. E.; Ogliaro, F.; Bearpark, M. J.; Heyd, J. J.; Brothers, E. N.; Kudin, K. N.; Staroverov, V. N.; Keith, T. A.; Kobayashi, R.; Normand, J.; Raghavachari, K.; Rendell, A. P.; Burant, J. C.; Iyengar, S. S.; Tomasi, J.; Cossi, M.; Millam, J. M.; Klene, M.; Adamo, C.; Cammi, R.; Ochterski, J. W.; Martin, R. L.; Morokuma, K.; Farkas, O.; Foresman, J. B.; Fox, D. J. *Gaussian 16 Rev. C.01*, Wallingford, CT, 2016.
91. Grimme, S.; Ehrlich, S.; Goerigk, L., Effect of the damping function in dispersion corrected density functional theory. *J. Comput. Chem.* **2011,** *32* (7), 1456-1465.
92. Weigend, F.; Ahlrichs, R., Balanced basis sets of split valence, triple zeta valence and quadruple zeta valence quality for H to Rn: Design and assessment of accuracy. *Phys. Chem. Chem. Phys.* **2005,** *7* (18), 3297-3305.
93. Glendening, E. D.; Landis, C. R.; Weinhold, F., NBO 6.0: Natural bond orbital analysis program. *J. Comput. Chem.* **2013,** *34* (16), 1429-1437.
94. Rahalkar, A.; Stanger, A. Aroma. https://chemistry.technion.ac.il/members/amnon-stanger/.
95. Gershoni-Poranne, R.; Stanger, A., The NICS-XY-Scan: Identification of Local and Global Ring Currents in Multi-Ring Systems. *Chem. Eur. J.* **2014,** *20* (19), 5673-5688.
96. Stanger, A., Obtaining Relative Induced Ring Currents Quantitatively from NICS. *J. Org. Chem.* **2010,** *75* (7), 2281-2288.
97. Becke, A. D., Density-functional thermochemistry. III. The role of exact exchange. *J. Chem. Phys.* **1993,** *98* (7), 5648-5652.
98. Lee, C.; Yang, W.; Parr, R. G., Development of the Colle-Salvetti correlation-energy formula into a functional of the electron density. *Phys. Rev. B* **1988,** *37* (2), 785-789.

SYNOPSIS TOC (Word Style "SN_Synopsis_TOC"). If you are submitting your paper to a journal that requires a synopsis graphic and/or synopsis paragraph, see the Instructions for Authors on the journal's homepage for a description of what needs to be provided and for the size requirements of the artwork.

To format double-column figures, schemes, charts, and tables, use the following instructions:

Place the insertion point where you want to change the number of columns
From the **Insert** menu, choose **Break**
Under **Sections**, choose **Continuous**
Make sure the insertion point is in the new section. From the **Format** menu, choose **Columns**
In the **Number of Columns** box, type **1**
Choose the **OK** button

Now your page is set up so that figures, schemes, charts, and tables can span two columns. These must appear at the top of the page. Be sure to add another section break after the table and change it back to two columns with a spacing of 0.33 in.

Table 1. Example of a Double-Column Table

Column 1	Column 2	Column 3	Column 4	Column 5	Column 6	Column 7	Column 8

Authors are required to submit a graphic entry for the Table of Contents (TOC) that, in conjunction with the manuscript title, should give the reader a representative idea of one of the following: A key structure, reaction, equation, concept, or theorem, etc., that is discussed in the manuscript. Consult the journal's Instructions for Authors for TOC graphic specifications.

Insert Table of Contents artwork here